J Biochem Technol (2024) 15(4): 17-25
https://doi.org/10.51847/cop0vCTgXX
ISSN: 0974-2328

QSAR, Docking Studies and in Silico Admet Prediction of 1,10-Phenanthrolinone Derivatives with Antitubercular Activities

Coulibaly Songuigama, Abdulrahim A. Alzain, Koné Soleymane, Deto U. Jean-Paul N'Guessan, Brigitte Gicquel, Christophe Rochais, Patrick Dallemagne, Mahama Ouattara*

Received: 16 September 2024 / Received in revised form: 07 December 2024, Accepted: 08 December 2024, Published online: 19 December 2024

Abstract

Research for new drugs to combat drug resistance in tuberculosis bacilli is one of the solutions to overcome this disease. In this sense, we have designed, synthesized, and fully characterized the chemical structures of about 20 derivatives of 1,10-phenanthrolinone. The evaluation of the antitubercular activities of Mycobacterium tuberculosis revealed that some of these compounds are highly active. Furthermore, the research of the structure-activity connection showed that the derivatives with the nitro group at C6, a carboxylic acid, ester, amide, or hydrazine-like function at C3, and a methyl or ethyl alkylated pyrrolic nitrogen atom at C3 had the best antitubercular activities. The QSAR studies undertaken showed that it is possible to establish a mathematical relationship between antitubercular activities and chemical structures. The obtained QSAR model highlighted that antitubercular activity was significantly affected by chemical softness (s), chemical hardness (η) and chemical potential (μ). In other words, substituents that increase the overall molecular reactivity of 1,10-phenanthrolinone will lead to good antitubercular activities. Furthermore, the prediction of ADMET properties showed that 1,10-phenanthrolinones possess good pharmacokinetic properties. Further, molecular docking confirmed the importance of the carboxylic acid chemical function in position 3 and the nitro group in position 6 for a good affinity of 6-nitro 1,10-phenanthrolinones with deazaflavin-dependent nitroreductase, chosen as a potential target.

Keywords: 1,10-phenanthrolinone Antitubercular activities, QSAR, ADMET, Molecular docking

Coulibaly Songuigama, Deto U. Jean-Paul N'Guessan, Mahama Ouattara*
Department of Therapeutic and Organic Chemistry, UFR Pharmaceutical and Biological Sciences, FHB University, 01 BP V34 Abidjan, Côte d'Ivoire.

Abdulrahim A. Alzain
Department of Pharmaceutical Chemistry, Faculty of Pharmacy, University of Gezira, Gezira, Sudan.

Koné Soleymane
Laboratory of Structural Organic Chemistry, UFR Structural Sciences of Matter and Technology, FHB University, 22 BP 582 Abidjan 22, Côte d'Ivoire.

Brigitte Gicquel
Department of Tuberculosis Control and Prevention, Shenzhen Nanshan Center for Chronic Disease Control, Shenzhen, China.

Christophe Rochais, Patrick Dallemagne
University of Normandie, UNICAEN, CERMN, Caen, 14000, France.

***E-mail:** mahama.ouattara@univ-fhb.edu.ci

Introduction

The infectious illness known as TB is spread by mycobacteria of the tuberculosis complex, primarily Koch's bacillus or Mycobacterium tuberculosis. Tuberculosis has existed for more than 120 centuries, and in 2018, the number of people affected was estimated to be around 10 million, with a morbidity that varies from country to country, ranging up to more than 500 new cases per 100,000 inhabitants per year (Cardona, 2018; WHO, 2023a). In the same year, the number of deaths due to TB was estimated at 1.2 million among HIV-negative people and 251,000 among HIV-positive people (Cardona, 2018; WHO, 2023a). The drug treatment of tuberculosis is based on a combination of several specific antibiotics or antitubercular drugs for at least six months (WHO, 2023a). However, although effective, TB treatment faces several obstacles, such as compliance, duration of treatment, adverse effects of TB drugs, management of latent tuberculosis with dormant bacilli, and the emergence of multidrug-resistant strains (Blanc *et al*., 2020; WHO, 2023a, 2023b). As stated by the World Health Organization (WHO), this drug resistance of bacilli to antitubercular drugs undermines the success of tuberculosis control (Blanc *et al*., 2020; WHO, 2023a, 2023b). In addition, the deadly combination of HIV and tuberculosis poses new diagnostic and therapeutic challenges. Faced with the emergence of multidrug-resistant strains and the drawbacks of current antitubercular drugs, WHO is encouraging the search for new compounds active on resistant strains and capable of sterilizing the sites where dormant bacilli persist while reducing the duration of treatment. It is in this context that we reported in a previous work the design, synthesis, and antitubercular activities of 1,10-phenanthrolinone derivatives (Coulibaly *et al*., 2020). To create a serial molecular model of the antitubercular 1,10-phenanthrolinones from the quantum descriptors using the DFT calculation method and the B3LYP/ 6-31+G (d,p) theory, we have conducted a quantitative structure-activity relationship (QSAR) study in this work. Additionally, Schrodinger's in silico qikprop

tool was used to assess the 24 compounds' in silico ADMET characteristics. Finally, the binding mode of the most potent compound was studied using molecular docking analysis.

Materials and Methods

Synthetic Chemistry

The chemical synthesis of 1,10-phenanthrolinone derivatives was performed in a previous work. The synthesis protocols, NMR spectra, mass spectra, IR spectra, LC-MS spectra, and melting points of all the obtained compounds have been described in this paper (Coulibaly *et al*., 2020).

Evaluation of Antitubercular Activities

At the end of the chemical synthesis, the 1,10-phenanthrolinone derivatives were evaluated for antitubercular activities on a strain of Mycobacterium tuberculosis on Sauton culture medium. This activity was performed in comparison to Rifampicin, Amikacin, and Ofloxacin by the resazurin reduction test at the Institut Pasteur from Paris. The protocols of the biological tests have been described in our previous article (Gicquel *et al*., 2019; Coulibaly *et al*., 2020).

QSAR and Theoretical Calculations

Level of Calculation

The Gaussian 09 program was used to carry out the computations (Frisch *et al*., 2009). In QSAR investigations, DFT techniques are well recognized to produce a range of molecular characteristics (Parr *et al*., 1978; Chattaraj *et al*., 1995; De Proft *et al*., 1996a, 1996b, 1996c; De Proft *et al*., 1997; Geerlings *et al*., 1998; Ayers *et al*., 2000). The B3LYP/6-31+G(d,p) level of theory optimization computation is used to identify all other descriptors, with the exception of lipophilicity, which was computed using KowWin/logP software. Regarding the modeling, XLSTAT (XLSTAT Version 19.5.47062 (64 bit) Copyright 1995-2018, 2018) and Excel (Microsoft ® Excel ® 2013 (15.0.4420.1017) MSO (15.0.4420.1017) 64 Bits, 2013) were used to develop the multilinear regression approach.

Quantic Descriptors

Electronic energy (Eelectr), HOMO energy (EHOMO), LUMO energy (ELUMO), energy gap (ΔE), chemical hardness (^{r}), chemical softness (S), electrophilicity (ω), chemical potential (μP), dipole moment (μd), lipophilicity (logP), ionization potential (PI), and electronic affinity (AE) were among the twelve theoretical descriptors that were computed in order to develop the QSAR model. By combining three of these characteristics, we were able to create a useful model. In addition to chemical potential, we also have chemical softness (S) and chemical hardness (^{r}). One measure of a molecule's reactivity is its chemical softness (Chattaraj *et al*., 1996). The stability of the molecule is indicated by its chemical hardness (η) (Xavier *et al*., 2015). The tendency of a molecular system to draw electrons to itself is explained at the chemical potential level. These distinct descriptors are independent of one another, as indicated by the partial correlation coefficient between the examined descriptors being less than 0.70 (aij ˆ 0.70) (Vessereau, 1988).

Estimation of the Predictive Capacity of a QSAR Model

Several metrics, including the standard deviation S, the correlation coefficients of the cross-validation Q2CV, the Fischer coefficient F, and the coefficient of determination R2, are used to assess a model's quality. The fit of estimated and experimental values is shown by the statistical indices R2, S, and F. They enable measuring the accuracy of the computed values on the training set and explain the prediction capacity within the model's bounds (Snedecor & Cochran, 1967). Information on the model's predictive ability is provided by the cross-validation coefficient. The dispersion of the theoretical values around the experimental values is shown by R2. The closer the points are to the fitting line, the higher the model quality (Esposito *et al*., 2004). The coefficient of determination may be used to assess how well the points match the line.

$$R^2 = 1 - \frac{\sum(y_{i,exp} - \hat{y}_{i,théo})^2}{\sum(y_{i,exp} - \bar{y}_{i,exp})^2} \quad (1)$$

$Y_{i,exp:}$ Experimental value of antitubercular activity
$\hat{y}_{i,théo:}$ Theoretical value of antitubercular activity
$\bar{y}_{i,exp:}$ Experimental mean value of antitubercular activity

The greater the correlation between the theoretical and experimental values, the closer the R^2 value is to 1. Furthermore, the connection 1 determines the variance σ^2.

$$\sigma^2 = S^2 = \frac{\sum(y_{i,exp} - y_{i,théo})^2}{n - k - 1} \quad (2)$$

N is the number of molecules in the test or training set, k is the number of independent variables (descriptors), and n-k-1 is the degree of freedom. The mean deviation another statistical indicator that is employed is S. It evaluates the model's accuracy and dependability.

$$S = \sqrt{\frac{\sum(y_{i,exp} - y_{i,théo})^2}{n - k - 1}} \quad (3)$$

Additionally, the Fischer F coefficient is used to assess the model's degree of statistical significance, or the caliber of the descriptor selection that goes into the model.

$$F = \frac{\sum(y_{i,théo} - y_{i,exp})^2}{\sum(y_{i,exp} - y_{i,théo})^2} * \frac{n - k - 1}{k} \quad (4)$$

The coefficient of determination of the cross-validation Q^2_{CV}, assesses the accuracy of the prediction on the test set and is calculated using the following equation.

The cross-validation Q^2_{CV} coefficient of determination, which is determined using the following formula, evaluates how accurate the prediction was on the test set.

$$Q^2_{cv} = \frac{\sum(y_{i,théo} - \bar{y}_{i,exp})^2 - \sum(y_{i,théo} - y_{i,exp})^2}{\sum(y_{i,théo} - \bar{y}_{i,exp})^2} \quad (5)$$

As stated by Eriksson *et al*. (2003), a model's performance is defined by a value of Q2CV > 0.5 for a decent model and more than 0.9 for an exceptional model. If the acceptance criterion R2-Q2CV < 0.3 is satisfied, the model's training set will demonstrate good performance. The value of the ratio log (1/MIC) theo/log(1/MIC) exp of the test set may also be used to determine a model's predictive potency. The model is deemed appropriate when the ratio of theoretical to experimental activity tends to Eq. 1.

In Silico ADMET Prediction and Molecular Docking

The druggable characteristics of the produced compounds were predicted using the Schrodinger suite's QikProp module. The pharmacokinetic characteristics and toxicity of the substances were evaluated. Additionally, the compounds were analyzed using Lipinski's rule of five.

Glide of Schrodinger's SP mode was used for molecular docking investigations, and Schrodinger's SiteMap was used to estimate the binding location.

Results and Discussion

Pharmacochemistry Section

The antitubercular results obtained are gathered in **Table 1**.

Table 1. Antimycobacterial activities [MIC90 (µM)] of 1,10-phenanthroline-3-carboxylic acid derivatives, rifampicin, ofloxacin, and amikacin on *M. tuberculosis*.

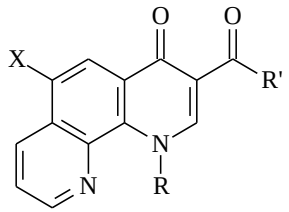

MIC_{90} (µM)

N°	R	R'	X	Sauton medium
1	H	OC_2H_5	H	23.99
2	CH_3	OC_2H_5	H	12.88
3	C_2H_5	OC_2H_5	H	25.15
4	H	OC_2H_5	NO_2	103.00
5	CH_3	OC_2H_5	NO_2	0.39
6	C_2H_5	OC_2H_5	NO_2	0.11
7	CH_3	OC_2H_5	Cl	6.51
8	C_2H_5	OC_2H_5	Cl	3.44
9	CH_3	OC_2H_5	Br	3.28
10	C_2H_5	OC_2H_5	Br	3.73
11	CH_3	OC_2H_5	NH_2	109.50
12	C_2H_5	OC_2H_5	NH_2	26.08
13	CH_3	OH	H	13.13
14	C_2H_5	OH	H	25.25
15	CH_3	OH	NO_2	0.10
16	C_2H_5	OH	Br	13.04
17	H	OH	H	27.00
18	CH_3	NHC_6H_5	H	101.00
19	C_2H_5	NHC_6H_5	H	107.00
20	CH_3	NH_2	NO_2	0.42
21	C_2H_5	NH_2	NO_2	0.39
22	CH_3	$NHNH_2$	NO_2	1.63
23	C_2H_5	$NHNH_2$	NO_2	3.22
24	C_2H_5	NHC_6H_5	NO_2	13.38
Rifampicine				0.76

Ofloxacine	3.46
Amikacine	0.46

The analysis of the antitubercular activities obtained **(Table 1)** and the structure-activity relationship studies undertaken make it possible to establish the extension of the number of rings of the quinolones by the addition of a third ring of the pyridine type. This led to compound 1 possessing intrinsic antitubercular activities with an MIC at 23.99 µM. The different structural variations undertaken around this compound 1 and the resulting antitubercular activities allow to establish that the presence of a nitro group in position 6 of compound 1 leads to a loss of antitubercular activities (compound 4). As for the presence of a methyl or ethyl group on the nitrogen in position 1 of compound 1, this leads to a slight improvement of the antitubercular activities sought (compounds 2 and 3). On the other hand, the concomitant presence of these two modulators, that is to say the nitro group in position 6 and the alkyl in position 1, leads to compounds with better antitubercular activities. Indeed, with respective MICs of 0.39 and 0.11 µM, the N_1-alkylated and 6-nitro derivatives (compounds 5 and 6) proved to be more efficient than compound 3. The concomitant presence of these two modulators proves to be essential for the improvement of antitubercular activities. In order to verify the importance of the nitro group, it was reduced to an aromatic amine while maintaining the N_1-alkylation by a methyl or ethyl group. The resulting 6-amino derivatives (compounds 11 and 12) all exhibited low antitubercular efficiencies compared to the corresponding 6-nitro derivatives. Such a result reveals the importance of the nitro moiety as modulator of the antitubercular performance in the chemical series of 1,10-phenanthrolinones. Moreover, the replacement of the nitro by a bromine or chlorine atom (compounds 7- 10) generally leads to an improvement of the antitubercular efficacy compared to compound 1. As for the transformation of the ester function into carboxylic acid, it showed that the concomitant presence of a bromine atom in position 6 and a carboxylic acid function in position 3 leads to a decrease of the antitubercular activities (compound 16). On the other hand, with the 6-nitro and N_1-alkylated derivatives, the hydrolysis of the ester function into carboxylic acid leads to an improvement or even a maintenance of the antitubercular activities (compounds 13 - 15). From our results, it appears that in a series of 6-nitro N_1-alkylated derivatives, the transformation of the ester function into primary amide functions (compounds 20 and 21) leads to the maintenance or even to an improvement of the antitubercular efficiency. This antitubercular performance almost superposable to those of ester derivatives shows the amide function can be replaced by an ester one in the induction and maintenance of antitubercular activities. Moreover, in the same series, the replacement of the primary amine function by a hydrazide function leads to derivatives (Compounds 22 and 23), more efficient than compound 1 but less efficient than their corresponding ester and acid analogues. On the other hand, the replacement of the ester function by a secondary amide function (compounds 18 and 19) leads to an accentuated loss of the antitubercular efficiency independently of the nature of the N1-alkylation of the nitrogen and of the nitration in position 6.

QSAR Part and Theoretical Calculations

Training and Validation Set

In **Table 2** are gathered the molecular descriptors associated with the antitubercular activity of the 24 molecules. As for **Table 3**, it represents the values of the partial correlation coefficients of the descriptors.

Table 2. Molecular descriptors associated with antitubercular activity

Compounds	Log(1/CMI)	$\varepsilon_{élect}$(Kj/mol)	logP	μ_D(Debye)	E_{HOMO}(eV)	E_{LUMO}(eV)	µ(eV)	η(eV)	s(Ev-1)	ω(eV)	ΔE(eV)	PI(eV)	AE(eV)
1	4.61	-2400031.46	2.33	7.76	-6.31	-2.31	-4.31	2.00	0.50	4.65	4.00	6.31	2.31
2	4.89	-2503205.34	2.88	7.99	-6.17	-2.20	-4.18	1.98	0.50	4.41	3.97	6.17	2.20
3	4.59	-2606441.06	3.37	8.05	-6.14	-2.20	-4.17	1.97	0.51	4.41	3.94	6.14	2.20
4	3.99	-2933235.46	2.15	8.07	-5.99	-5.27	-5.63	0.36	2.77	44.01	0.72	5.99	5.27
5	6.41	-3040139.47	2.70	10.75	-6.70	-3.16	-4.93	1.77	0.56	6.86	3.54	6.70	3.16
6	6.96	-2606496.63	3.19	7.64	-6.17	-3.16	-4.66	1.50	0.67	7.23	3.01	6.17	3.16
7	5.19	-2296766.78	3.52	8.71	-6.26	-2.41	-4.34	1.93	0.52	4.87	3.86	6.26	2.41
8	5.46	-2193592.95	4.01	8.24	-6.24	-2.41	-4.32	1.91	0.52	4.88	3.83	6.24	2.41
9	5.48	-2833699.68	3.77	7.45	-5.47	-4.81	-5.14	0.33	3.05	40.30	0.66	5.47	4.81
10	5.43	-2193592.95	4.26	8.76	-6.23	-2.41	-4.32	1.91	0.52	4.89	3.82	6.23	2.41
11	3.96	-2647820.62	1.96	13.24	-5.63	-2.14	-3.88	1.75	0.57	4.31	3.50	5.63	2.14

12	4.58	-2751797.38	2.45	7.90	-5.66	-2.12	-3.89	1.77	0.56	4.26	3.55	5.66	2.12
13	4.88	-2296766.78	2.10	8.41	-6.30	-2.30	-4.30	2.00	0.50	4.62	4.00	6.30	2.30
14	4.6	-2193592.95	2.59	8.24	-6.45	-2.41	-4.43	2.02	0.50	4.87	4.04	6.45	2.41
15	7	-2833699.68	1.92	10.56	-6.84	-3.26	-5.05	1.79	0.56	7.11	3.58	6.84	3.26
16	4.89	-9150729.84	3.48	8.97	-6.35	-2.51	-4.43	1.92	0.52	5.11	3.84	6.35	2.51
17	4.57	-2193592.95	1.55	8.24	-6.45	-2.41	-4.43	2.02	0.50	4.87	4.04	6.45	2.41
18	4	-2851263.71	4.09	7.51	-6.08	-2.12	-4.10	1.98	0.50	4.25	3.96	6.08	2.12
19	3.97	-2950812.89	4.58	10.30	-5.42	-4.85	-5.13	0.29	3.46	45.55	0.58	5.42	4.85
20	6.38	-2781586.71	1.64	6.78	-6.86	-3.27	-5.06	1.79	0.56	7.14	3.59	6.86	3.27
21	6.41	-2884822.90	2.13	6.94	-6.83	-3.25	-5.04	1.79	0.56	7.09	3.58	6.83	3.25
22	5.78	-2926794.40	1.28	6.56	-6.57	-3.11	-4.84	1.73	0.58	6.77	3.46	6.57	3.11
23	5.49	-3030020.59	1.77	6.78	-6.53	-3.09	-4.81	1.72	0.58	6.73	3.43	6.53	3.09
24	4.87	-3030031.66	4.39	6.89	-6.55	-3.09	-4.82	1.73	0.58	6.73	3.45	6.55	3.09

Table 3. Values of the partial correlation coefficients of the descriptors

	μ(eV)	**s(Ev-1)**	**η(eV)**
μ(eV)	1	0.336	0.486
s(ev^{-1})	0.336	1	-0.967
η(eV)	0.486	-0.967	1

Between the descriptions, the partial correlation aij is less than 0.70. This demonstrates the descriptors' independence inside the model.

Validation of the QSAR Model

The sign of a descriptor's coefficient and its own sign both affect how much it contributes to TB activity with respect to other descriptors in the regression equation. The biological activity is enhanced by the descriptor when the sign and its coefficient are the same. Conversely, the descriptor reduces the activity if their signs are opposite. Based on the information in **Table 2**, the optimal model is shown in Eq. 6 below.

$$log\left(\frac{1}{CMI}\right) = 2.45 - 3\eta - 2.21\mu - 2.51S \quad (6)$$

η and μ en (eV); S en (eV^{-1})
R^2 = 0.900; Q^2 = 0.786; F= 36.18; S= 0.343; N= 16; R^2 - Q^2_{CV} = 0.114

Chemical softness, chemical potential, and chemical hardness are the three (03) characteristics that are elevated in this model. The cross-validation coefficient (Q2CV), Fischer's coefficient (F), and R2-Q2CV values demonstrate that the model in Eq. 6 is appropriate. In order to validate the model externally, chemicals 7, 8, 10, 12, 19, 21, and 24 were used.

A strong connection between the theoretical and experimental TB activity of the molecules under study is shown by the Log(1/c)Theo/Log(1/c)exp ratio values being near 1. **Figure 1** displays the regression line between the test set's (red dots) and training set's (blue dots) experimental and theoretical TB activity.

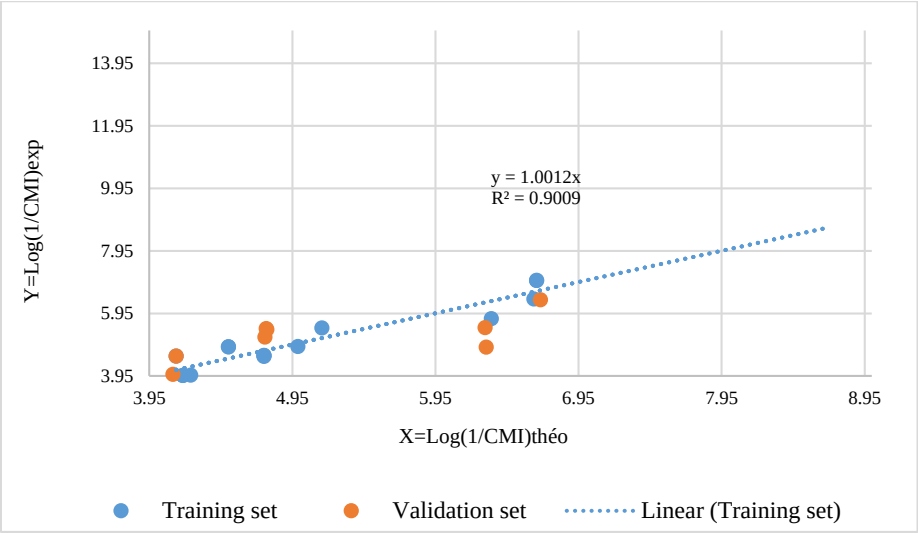

Figure 1. Plot between actual and predicted biological activity for the entire training and model validation set.

Analysis of the Contribution of Descriptors in the Model

The **Figure 2** below presents the coefficients (sign and importance) assigned to these descriptors.

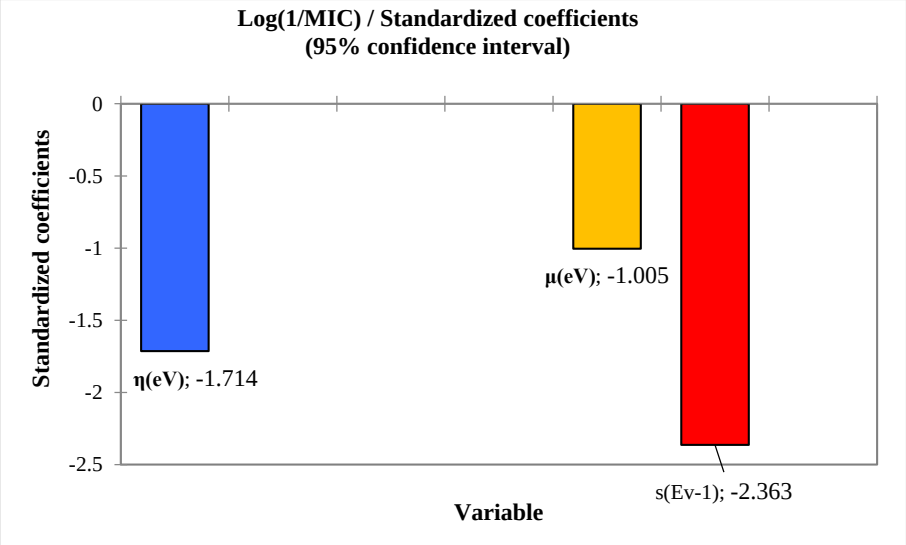

Figure 2. Coefficients defining the contributions of the three descriptors in antitubercular activity in the model.

Softness (s), hardness (η), and chemical potential (μ) are characteristics that show how reactive molecules are overall. The capacity of a chemical entity to give or receive electrons is expressed by its hardness (η) and softness (s), while its chemical potential (μ) indicates its propensity to attract electrons. A soft molecule will therefore have limited kinetic stability and strong chemical reactivity. Stated differently, molecules with a high hardness are stable and, as a result, less reactive chemically. Additionally, the chemical hardness and chemical potential are important markers of a molecule's overall reactivity since they show how well it can take in electrons (Abdel-Hadi *et al*., 2022; Elshorbagy *et al*., 2022; Nakagawa *et al*., 2022; Radhi *et al*., 2022; Rohmani *et al*., 2022). The characteristics of a good electrophile are low chemical hardness and high chemical potential. Because the coefficients of hardness (η) and softness (s) in our chemical series are negative, large values of these will enhance biological activity. Additionally, the low values of the chemical potential (μ) will help to increase biological activity. These results reveal that the 1,10-phenanthrolinone derivatives that exhibited the best antitubercular activities are those with better chemical reactivity. It seems that the N-alkylation of the nitrogen atom in position 1 and the C6 substitution of the tricycle by electron-withdrawing groups of nitro (NO_2) or halogen (bromine and chlorine) type leads to an improvement of the chemical reactivity of the 1,10-phenanthrolinone tricycle. Moreover, the nitro group being more electron-withdrawing than the halogen atoms, this translates

biologically into better antitubercular activity of the 6-nitro derivatives. In view of the above, one could think that a good reactivity of 1,10-phenanthroline derivatives is essential to establish the necessary interactions (van der Waals or hydrogen bonds or ionic bonds...) at the level of the biological target of *Mycobacterium tuberculosis*. Indeed, biological targets being of peptide nature, a good ligand-target or ligand-receptor interaction is conditioned by a good chemical reactivity of the ligand towards its target (Graham, 2017).

In Silico ADMET Prediction

Using the Schrodinger suite's QikProp module, the ADMET characteristics of the 24 1,10-phenanthrolinones with antitubercular activity were predicted **(Table 4)**. The permissible ranges for blood-brain barrier permeability (QplogBB) and water solubility (QplogS) are all met by all compounds. The majority of compounds exhibited superior permeability to MDCK cells. The cardiac toxicity of compounds 13–17 was modest (QPlogHERG). The 24 compounds' overall oral absorption percentage in humans varied between around 55 and 100 percent. There were no compounds that broke Lipinski's criterion of five.

Table 4. ADMET properties of the 1,10-phenanthrolinone derivatives with antitubercular activities.

Compounds	QPlogS[1]	QPlogHERG[2]	QPlogBB[3]	QPPMDCK[4]	Percent Human Oral Absorption[5]	Rule of Five
1	-3.319	-5.21	-0.69	327.867	90.473	0
2	-3.139	-5.153	-0.385	717.691	96.189	0
3	-3.38	-5.151	-0.45	720.066	100	0
4	-3.039	-4.935	-1.544	44.237	71.31	0
5	-3.044	-4.884	-1.241	96.832	77.319	0
6	-3.1	-4.888	-1.313	97.153	78.869	0
7	-3.754	-5.047	-0.23	1637.931	100	0
8	-4.011	-5.059	-0.298	1640.597	100	0
9	-3.862	-5.07	-0.219	1761.39	100	0
10	-4.119	-5.081	-0.287	1764.281	100	0
11	-3.549	-5.021	-0.956	201.944	83.92	0
12	-3.735	-5.02	-1.025	202.612	85.621	0
13	-2.385	-2.701	-0.738	53.043	74.15	0
14	-2.987	-2.823	-0.819	54.882	76.558	0
15	-2.105	-2.437	-1.526	7.157	54.987	0
16	-3.7	-2.731	-0.673	130.37	79.198	0
17	-2.565	-2.76	-1.016	24.232	68.433	0
18	-4.504	-6.382	-0.381	789.241	100	0
19	-4.746	-6.38	-0.442	802.741	100	0
20	-2.743	-4.262	-1.569	22.438	62.009	0
21	-3.003	-4.378	-1.661	23.583	64.138	0
22	-2.961	-4.503	-1.922	12.36	56.646	0
23	-3.197	-4.608	-2.017	12.991	58.713	0
24	-4.465	-6.118	-1.341	108.308	87.136	0

[1] Predicted aqueous solubility in mol/L (acceptable range -6.5–0.5).
[2] log HERG, HERG K+channel blockage (concern below -5)
[3] Predicted blood brain barrier permeability (acceptable range -3–1.2).
[4] Predicted apparent MDCK cell permeability in nm/s (acceptable range in nm/s (acceptable range: <25 is poor and >500 is great). MDCK cells are a good model for the blood–brain barrier
[5] Percentage of human oral absorption (acceptable range: <25 is poor and >80% is high.

Molecular Docking Studies

In order to identify the hypothetical binding modes of the most potent molecule 15, the molecule was anchored in the binding cavity of the deazaflavin-dependent nitroreductase from Mycobacterium tuberculosis (PDB ID: 3r5L) using Schrodinger's 2021 suite.

The choice of this nitroreductase is justified by the fact that it is involved in the bioactivation of pretomanid, an antituberculosis agent that is also nitrous like the phenanthrolinones. The protein was prepared using Schrodinger's protein preparation assistant. As there is no ligand co-crystallized with the protein, the binding cavity was predicted using Schrodinger's SiteMap, which displayed a high site score and Dscore of 0.99 and 0.81, respectively, as shown in **Table 5**. This binding site contains amino acid residues that have previously been reported in the binding of 3r5L and PA-824, confirming the reliability of the predicted binding cavity

Table 5. Binding cavity site parameters predicted using SiteMap.

Site	SiteScore	Size	Dscore	volume	residues
Site 1	0.99	119	0.806	242.844	Chain E: 17,46,53,54,55,56,60,62,63,64,65,76,77,78,79,86,87,88,90,91,130,133,136,154,161,168,315,383,413,415,420

The docking study of the most active molecule 15 revealed a good fit in the binding site with four hydrogen bonding interactions with the amino acids LYS79 and MET87 and water in the active site. In addition, this compound formed hydrophobic interactions in the binding site. In addition, the compound exhibited high negative scores of -6.210 kcal/mol, indicating good binding affinity to deazaflavin-dependent nitroreductase. Furthermore, docking confirmed the importance of the carboxylic acid chemical function in position 3 and the nitro group in position 6. These seem to be essential for a good affinity of the 6-nitro 1,10-phenanthrolinones with the biological target.

Conclusion

The leading cause of infectious-origin death worldwide is pulmonary TB. In this instance, Mycobacterium tuberculosis is the bacillus that causes it. In addition to the lengthy course of treatment, the bacilli's resistance to the majority of medications makes therapeutic management of this illness more difficult. A synergistic combination of many antitubercular medications has been suggested as a control method to deal with this. However, the hunt for novel and more potent compounds is crucial given the rise of ultra-resistant strains. It is in this context that we have designed, prepared, and evaluated new 1,10-phenanthrolinone derivatives as potential new antitubercular drugs. Antibacillary screening of the latter on Mycobacterium tuberculosis revealed excellent antituberculosis activities for some of them, especially those nitrated at position 6. Indeed, with activities ranging between 0.10 and 0.42 μM, the 6-nitro-phenanthrolinones proved to be particularly effective on Mycobacterium tuberculosis. There was a strong agreement between the theoretical and experimental antitubercular activity of the molecules, according to QSAR studies conducted to relate the antitubercular activities to the chemical profile of 1,10-phenanthrolinones. Consequently, improved antitubercular activities are a result of increased chemical softness (S), chemical hardness (η), and chemical potential (μ), all of which indicate improved total molecular reactivity. Finally, using the example of electron-withdrawing groups, QSAR demonstrated that substituents in position 6 of the tricycle can be used to predict and, in particular, increase the antitubercular activities of 1,10-phenanthrolinones by increasing the molecules' overall reactivity. QikProp analysis of the 24 compounds' pharmacokinetic properties demonstrated the hit compounds' drug-like characteristics. Moreover, molecular docking studies revealed key hydrogen bonding interactions between the most active compound 15 and Deazaflavin-dependent nitroreductase of *Mycobacterium tuberculosis*.

Acknowledgments: None

Conflict of interest: None

Financial support: None

Ethics statement: None

References

Abdel-Hadi, B., & Abdel-Fattah, S. R. (2022). Clinical pharmacist intervention in Appendectomy - Dexmedetomidine as an adjunct therapy. *Journal of Advanced Pharmacy Education and Research, 12*(2), 1-5. doi:10.51847/AYOZXtLMrj

Ayers, P. W., & Parr, R. G. (2000). Variational principles for describing chemical reactions: The Fukui function and chemical hardness revisited. *Journal of the American Chemical Society*, *122*(9), 2010-2018. doi:10.1021/ja9924039

Blanc, F. X., Badje, A. D., Bonnet, M., Gabillard, D., Messou, E., Muzoora, C., Samreth, S., Nguyen, B. D., Borand, L., Domergue, A., et al. (2020). Systematic or test-guided treatment for tuberculosis in HIV-infected adults. *New England Journal of Medicine*, *382*(25), 2397-2410. doi:10.1056/NEJMoa1910708

Cardona, P. J. (2018). Patogénesis de la tuberculosis y otras micobacteriosis. *Enfermedades infecciosas y microbiologia clinica*, *36*(1), 38-46. doi:10.1016/j.eimc.2017.10.015

Chattaraj, P. K., Cedillo, A., & Parr, R. G. (1995). Variational method for determining the Fukui function and chemical hardness of an electronic system. *The Journal of Chemical Physics*, *103*(17), 7645-7646. doi:10.1063/1.470284

Chattaraj, P. K., Cedillo, A., & Parr, R. G. (1996). Chemical softness in model electronic systems: Dependence on temperature and chemical potential. *Chemical Physics*, *204*(2-3), 429-437. doi:10.1016/0301-0104(95)00276-6

Coulibaly, S., Cimino, M., Ouattara, M., Lecoutey, C., Buchieri, M. V., Alonso-Rodriguez, N., Briffotaux, J., Mornico, D., Gicquel, B., Rochais, C., et al. (2020). Phenanthrolinic analogs of quinolones show antibacterial activity against M.

tuberculosis. *European Journal of Medicinal Chemistry*, *207*, 112821. doi:10.1016/j.ejmech.2020.112821

De Proft, F., & Geerlings, P. (1997). Calculation of ionization energies, electron affinities, electronegativities, and hardnesses using density functional methods. *The Journal of Chemical Physics*, *106*(8), 3270-3279. doi:10.1063/1.473796

De Proft, F., Martin, J. M. L., & Geerlings, P. (1996a). Recent developments in density functional theory. In: J. Seminario (Ed.), *Theoretical and Computational Chemistry* (Vol. 4, p. 773), Amsterdam: Elsevier.

De Proft, F., Martin, J. M., & Geerlings, P. (1996b). On the performance of density functional methods for describing atomic populations, dipole moments and infrared intensities. *Chemical Physics Letters*, *250*(3-4), 393-401. doi:10.1016/0009-2614(96)00057-7

De Proft, F., Martin, J. M., & Geerlings, P. (1996c). Calculation of molecular electrostatic potentials and Fukui functions using density functional methods. *Chemical Physics Letters*, *256*(4-5), 400-408.

Diudea, M. V. (2000). QSPR/QSAR studies for molecular descriptors. Nova Science, Huntingdon, New York, USA.

Elshorbagy, R. T., Balbaa, A. E. A., Ayad, K. E., Allam, N. M., Eladl, H. M., & Allah, W. R. A. (2022). Cognitive task versus focus of attention on dynamic postural control in recurrent ankle sprains. *Journal of Advanced Pharmacy Education and Research*, *12*(2), 6-10. doi:10.51847/OYUrFadR58

Eriksson, L., Jaworska, J., Worth, A. P., Cronin, M. T., McDowell, R. M., & Gramatica, P. (2003). Methods for reliability and uncertainty assessment and for applicability evaluations of classification-and regression-based QSARs. *Environmental Health Perspectives*, *111*(10), 1361-1375. doi:10.1289/ehp.5758

Esposito, E. X., Hopfinger, A. J., & Madura, J. D. (2004). Methods for applying the quantitative structure-activity relationship paradigm. *Methods in Molecular Biology*, *275*, 131-214. doi:10.1385/1-59259-802-1:131

Frisch, M. J., Trucks, G. W., Schlegel, H. B., Scuseria, G. E., Robb, M. A., Cheeseman, J. R., Scalmani, G., Barone, V., Mennucci, B., Petersson, G. A. H., et al. (2009). Gaussian 09, Revision A.02. Gaussian, Inc., Wallingford.

Geerlings, P., De Proft, F., & Langenaeker, W. (1998). Density functional theory: A source of chemical concepts and a cost-effective methodology for their calculation. *In: Advances in Quantum Chemistry* (Vol. 33, pp. 303-328). Academic Press. doi:10.1016/S0065-3276(08)60442-6

Gicquel, B., Cimino, M., Dallemagne, P., Rochais, C., Coulibaly, S., & Ouattara, M. (2019). Phenanthrolinone derivatives for use in the treatment of bacterial infections. U.S. Patent N° WO2019138084 (A1). Accessed from: https://worldwide.espacenet.com/publicationDetails/biblio?II=0&ND=3&adjacent=true&locale=en_EP&FT=D&date=20190718&CC=WO&NR=2019138084A1&KC=A1

Graham, P. L. (2017). *An Introduction to Medicinal Chemistry*. Oxford University Press.

Microsoft ® Excel ® 2013 (15.0.4420.1017) MSO (15.0.4420.1017) 64 Bits (2013) Part of Microsoft Office Professional Plus.

Nakagawa, N., & Yamashita, T. (2022). Comparative study of traditional face-to-face teaching, audience response system, and a flipped classroom plus audience response. *Journal of Advanced Pharmacy Education and Research*, *12*(1), 9-16. doi:10.51847/ODLhsGztZ9

Parr, R. G., Donnelly, R. A., Levy, M., & Palke, W. E. (1978). Electronegativity: The density functional viewpoint. *The Journal of Chemical Physics*, *68*(8), 3801-3807. doi:10.1063/1.436185

Radhi, A. A., & Jaafar, I. S. (2022). Factors influencing the dissolution behavior of meloxicam dispersions. *Journal of Advanced Pharmacy Education and Research*, *12*(3), 9-14. doi:10.51847/7qrSvPhtkH

Rohmani, S., Desi, B. A., & Wardhani, W. D. (2022). Potassium-Azeloyl-Diglycinate BB-Cream formulation with Triethanolamine variation, and its effects on In-Vitro SPF stability and values. *Journal of Advanced Pharmacy Education and Research*, *12*(1), 1-8. doi:10.51847/MUHp4ptold

Snedecor, G. W., & Cochran, W. G. (1967). Statistical Methods. Oxford and IBH, New Delhi, India.

Vessereau, A. (1988). Méthodes statistiques en biologie et en agronomie. Lavoisier (Tec & Doc). Paris.

WHO. (2023a). Global tuberculosis report 2020: Executive summary. Available from: https://apps.who.int/iris/bitstream/handle/10665/336069/9789240013131-eng.pdf

WHO. (2023b). Guidelines for treatment of tuberculosis. 4th ed. Available from: https://www.who.int/tb/publications/2010/9789241547833/en/

Xavier, S., Periandy, S., & Ramalingam, S. (2015). NBO, conformational, NLO, HOMO–LUMO, NMR and electronic spectral study on 1-phenyl-1-propanol by quantum computational methods. *Spectrochimica Acta Part A: Molecular and Biomolecular Spectroscopy*, *137*, 306-320. doi:10.1016/j.saa.2014.08.039

XLSTAT Version 19.5.47062 (64 bit) Copyright 1995-2018 (2018) XLSTAT and Addinsoftware Registrered Trademarks of Addinsoft. Available from: https: //www.xlstat.com